ELSEVIER

Ceramics International 28 (2002) 355–362

CERAMICS INTERNATIONAL

www.elsevier.com/locate/ceramint

The effect of powder processing on densification, microstructure and mechanical properties of hydroxyapatite

Nithyanantham Thangamani[a,*], Kandasamy Chinnakali[b], F.D. Gnanam[a]

[a]*Centre for Ceramic Technology, Anna University, Chennai 600 025, India*
[b]*Department of Physics, Anna University, Chennai 600 025, India*

Received 12 January 2001; received in revised form 28 January 2001; accepted 2 September 2001

Abstract

The influence of powder processing and sintering temperature on densification, microstructure and mechanical properties of hydroxyapatite (HAp) ceramics was studied. The as-dried, calcined and processed HAp powders were uniaxially compacted and sintered at various temperatures (1000–1400 °C) for 3 h. The as-dried and processed powders, attained 97% of theoretical density (TD) at 1100 °C; at higher sintering temperatures, the density of the as-dried powder compact was found to decrease. A uniform microstructure with fine grain size (2.3 μm) was observed for material obtained from processed powder, whereas exaggerated grain growth with closed pores were observed in as-dried and unprocessed powder compacts. The Vickers' hardness, fracture toughness and flexural strength of HAp were determined and a maximum value of 6.3 GPa and 0.88 $MPam^{\frac{1}{2}}$ and 60.3 MPa, respectively were obtained for processed compact. The processing of HAp has improved its densification, microstructure homogeneity and mechanical properties.

Keywords: A. Sintering; C. Mechanical properties; D. Apatite; E. Biomedical applications

1. Introduction

Development of dense hydroxyapatite (HAp) ceramics with superior mechanical properties is possible if the starting powder is stoichiometric with better powder properties like particle size, distribution and morphology [1,2]. Synthetic HAp can be pressurelessly sintered up to theoretical density (T.D) at moderate temperatures (1000–1200 °C) [3–5]. The fabrication of fine grained HAp ceramics without the assistance of applied pressure demands control over the powder properties since many strength limiting microstructural heterogeneities stem from the powder itself. The important methods for the preparation of HAp powder are solid state reaction, precipitation and hydrolysis of calcium phosphates. All these methods are capable of producing agglomerates either during reaction or drying and agglomerates are a major heterogeneity in powders. Agglomerates with different bulk densities can persist during powder consolidation to form crack-like voids during densification because of their different shrinkage rates relative to the surrounding powder compact. Moreover, the wide particle size distribution of the powder with irregular morphology causes poor packing, which results in exaggerated grain growth during sintering. These microstructural heterogeneities seriously affect the mechanical properties of the sintered HAp. Hence, the processing of HAp before consolidation is very essential to obtain agglomerate free, fine powders with spherical morphology.

Few studies have been reported on the development of fine HAp powders with spherical morphology, however, limited reports on the effect of powder properties like, particle size, distribution, density and morphology on the densification behaviour, mechanical and microstructural characteristics of those powder compacts are available [6–10]. The sintering temperature for dense HAp strongly depends on the powder properties and powder packing. Therefore, a processing method was designed to improve and control the powder properties such as crystallinity, particle size, particle size distribution and powder morphology. The processing method was three fold; calcination (to improve the crystallinity), rehydration (to restore the water) and communition (to

* Corresponding author at present address: Department of Metallurgy, Indian Institute of Science, Bangalore-560 012, India.
E-mail address: ntmani@platinum.metalrg.iisc.ernet.in (N. Thangamani).

0272-8842/02/$22.00
PII: S0272-8842(01)00102-X

reduce the particle size, narrow the distribution and alter the powder morphology). This paper reports the results of a systematic study on the influence of powder processing and sintering temperatures on densification behaviour, microstructure development and mechanical properties of HAp.

2. Experimental procedure

The HAp was prepared by the precipitation method [11]. The powder was calcined at two different temperatures, 800 and 1000 °C for 3 h. Subsequently, a portion of the calcined powders were rehydrated for 48 h by dispersing in double distilled water. The rehydrated powder was milled in propanol medium by employing a planetary mill with a powder, propanol ratio of 1:1. Stearic acid (1.0 wt.%) was used as a lubricant during milling. All the powders were characterized with XRD (Siemens D-5000 X-ray diffractometer), FTIR (Bruker IFS 66V) and TG/DTA (Metler Toledeo Stare system). The particle size of the powders was analyzed by using a laser diffraction particle size analyzer (Shimadzu, SALD 1100) and scanning electron microscopy (Leica Stereoscan 440, Cambridge) was used to evaluate the powder morphology. The powder density was determined by the Archimedes' method.

The as-dried HAp powder (AD), and 800 and 1000 °C calcined and processed powders were uniaxially pressed at 65 MPa into pellets (10 mm diameter) and bars (60×5.0×5.0 mm). For lubrication, the interior surface of the dies were coated with a layer of stearic acid. The green compacts were sintered at various temperatures ranging from 1000 to 1400 °C in air. The heating rate was 2 °C/min up to 800 °C and after a soaking period of 30 min at 800 °C, the heating rate was increased to 5 °C/min up to the sintering temperature. The dwelling time was 3.0 h and the cooling was performed at the rate of 2 °C/min. Density of the sintered compacts was measured by the Archimedes' method. The shrinkage of the compacts was also measured. The microstructural and fracture surface analysis of the sintered HAp composites were carried out by using an optical microscope (Leica) and SEM. For this, the sintered compacts were lapped and polished using various grades of silicon carbide papers (grade 400–1200) and diamond paste of 1.0 μm was used to do the final polishing. Lactic acid (0.15 M, pH = 2.4) was used as an etchant to reveal the microstructure of the sintered compact. The etched surfaces and fracture surfaces were coated with gold films before the microstructure analysis. The average grain size was found by using the linear intercept method.

The Vickers' hardness of the HAp compacts was measured by using Zwick (3212) hardness tester. The indentations were performed on the polished surfaces at various testing loads between 1.96 and 9.80 N with an indentation time of 30 s. Higher loads were avoided because they resulted in extensive cracking. The fracture toughness (K_{IC}) of the samples was determined by using the indentation technique by measuring the crack length and using known equations [12]. The flexural strength of unpolished specimens at room temperature was obtained by 3-point bending test using a Zwick universal testing machine (1445). The span length was 20 mm and the cross head speed was 0.5 mm/min. Six specimens were tested and the average was reported in all tests.

3. Results and discussion

3.1. Powder properties

The results of TG/DTA, XRD and FT–IR analysis showed that the HAp is crystalline and phase pure. No mechonochemical effect due to milling of the powder was observed which has been discussed by the authors elsewhere [13]. The powder properties are given in Table 1. The calcination reduces the particle size and narrows the size distribution. The rehydration and milling of the powder further reduces the particle size and distribution and a fine powder (800P) with an average particle size of 1.0 μm is obtained. The SEMs of the AD, 800P and 1000P powders are shown in Fig. 1. The AD powder consists of hard agglomerates which are irregular in shape composed of fine crystallites. The 800P powder exhibits a spherical morphology, and in this soft granules

Table 1
Effect of processing on crystallite size, particle size and powder density of HAp

Sample	Processing conditions	Crystallite size[a] (nm)	Particle size[b] (μm)			Powder denisity (g/cc)
			d_{90}	d_{50}	d_{10}	
AD	As-dried	28.00	34.79	14.85	3.12	2.16
800C	Calcined at 800 °C for 3 h	36.00	7.9	3.03	1.49	2.65
800P	Calcined at 800 °C and milled for 6 h	36.00	3.28	1.0	0.49	2.77
1000C	Calcined at 1000 °C for 3 h	40.00	16.8	7.58	2.66	2.67
1000P	Calcined at 1000 °C and milled for 6 h	41.00	3.89	2.77	0.81	2.82

[a] XRD analysis.
[b] Laser diffraction method.

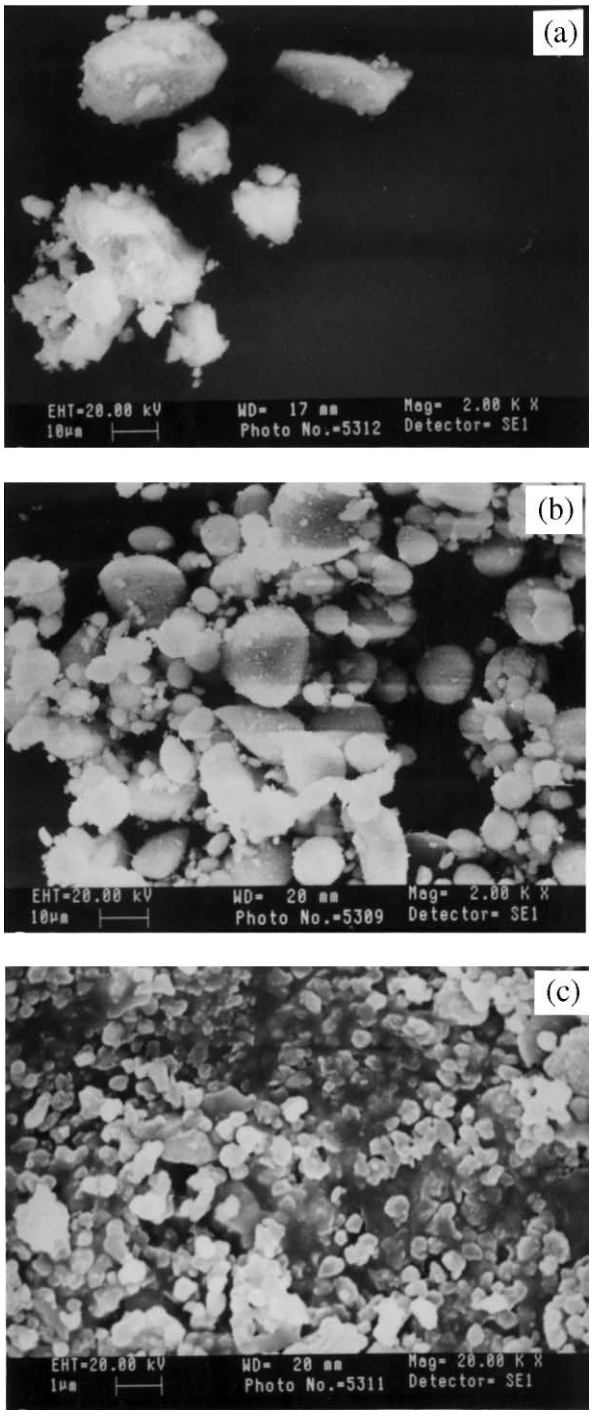

Fig. 1. SEM micrographs of (a) AD, (b) 800P and (c) 1000P HAp powders.

the particles are held together by short range surface forces. These forces may be electrostatic and van der Waal's attractions between particles or liquid capillary forces due to presence of liquid within the granules. The agglomerates found in the 1000P powder are due to the initial stage of sintering, hence, they are hard and small in size.

3.2. Densification studies

The variation of sintered density with sintering temperature for all HAp samples is shown in Fig. 2. Both the AD and 800P powder compacts attain a maximum sintered density of 97% of TD at 1100 °C whereas, the 1000P gets densified at 1300 °C with 97.4% of T.D. On the other hand, the 800 and 1000 °C powders attain their maximum density only at 1200 and 1350 °C, respectively. After reaching a maximum value, the sintered densities of all powder compacts except AD reach a plateau at higher sintering temperatures. At higher sintering temperatures, the densification rate is high and the compacts exhibit moderate to high grain growth. Any difference in initial grain sizes generate forces on the grain boundaries that cause grain growth. As the temperature is increased, the rate of grain boundary motion increases and breakaway of the boundaries from the pores and leaving of isolated pores in the grain interior occurs because the pores are slower moving than the grain boundaries [14]. Under the tension of a moving grain boundary, pores can move by volume or surface diffusion or even by evaporation–condensation across the pores, but this requires close control of the heating rate to keep the pores along with the grain boundaries [15]. The pores formed by the irregular powder species of AD cannot be completely removed by rapid sintering rate and remain as closed pores which limits the final density. Usually, another possible reason for this reduced density at higher sintering temperature would be the decomposition of HAp into other calcium phosphates. In this investigation, the sintered AD, 800P and 1000P were analyzed by XRD and no decomposition was observed even at the sintering temperature of 1400 °C. The shrinkage of the HAp samples was measured and the AD powder compact shows a maximum shrinkage of 24% and that for the 800P and 1000P is 20 and 12%, respectively.

3.3. Microstructure analysis

Fig. 3 shows the optical micrograph of the as-dried, calcined and processed HAp ceramics sintered at temperatures ranging from 1100 to 1400 °C. Table 2 shows the average grain size of the HAp ceramics sintered at various temperatures. The AD compacts show non-uniform microstructures at 1100 °C and at higher sintering temperatures the formation of closed pores are also observed [Fig. 3(a–d)]. The micrographs of the 800C compact, sintered at 1100, 1200, 1300 and 1400 °C are shown in Fig. 3(e–h), respectively. The average grain size of 800C is 5.4 μm at 1100 °C but at 1400 °C, it is increased to 12.1 μm. A uniform microstructure exhibited by 800P sintered at the temperatures 1100–1400 °C are shown in Fig. 3(i–l). The average grain size of 800P at 1100 °C is 2.3 μm and a gradual grain growth is

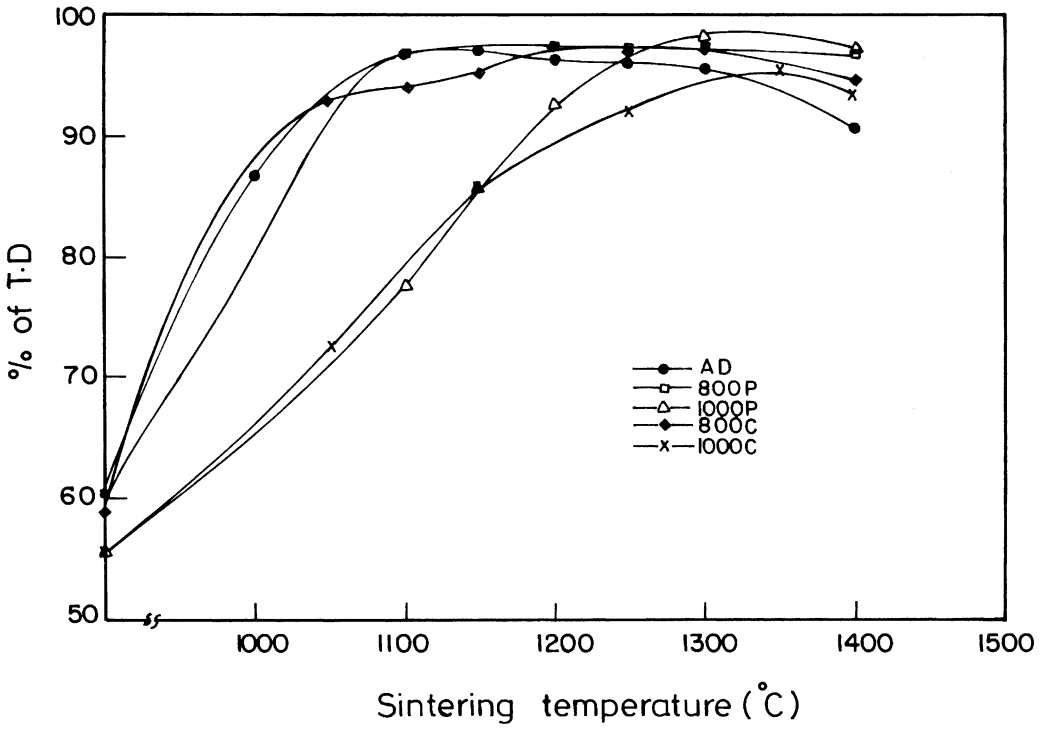

Fig. 2. Variation of sintered density with sintering temperature of HAp powder compacts.

Table 2
Average grain sizes of the HAp ceramics sintered at various temperatures

Sample	Sintering temperature (°C)			
	1100	1200	1300	1400
AD	1.2	2.3	3.3	16.0
800C	5.4	7.3	13.7	12.1
800P	2.3	2.4	3.74	10.06
1000C	–	–	9.3	18.13
1000P	–	–	5.86	10.29

observed with an increase in the sintering temperature. From the micrograph of 1000C, shown in Fig. 3(m and n), it is observed that 1000C at 1300 °C contains many open pores at the boundaries and grain junctions; few closed pores are also found within the grains. At 1300 °C, the grains of 1000P are fairly uniform and few pores remain at the grain boundaries and grain junctions; at 1400 °C, grain growth with very few closed pores is noted with an average grain size of 10.29 μm [Fig. 3(o and p)].

From these studies, it is clear that the as-dried and unprocessed powders favour the development of non-uniform grain structures. A wide distribution in particle size of the starting powder tends to promote a non-uniform grain structure at 1100 °C. This difference in initial grain size generate forces on the grain boundaries that cause abnormal grain growth at higher sintering temperatures. Grains larger than twice the critical size may develop abnormally due to the large driving force from highly curved boundaries [Fig. 3(h)] between the large grain and the matrix [16]. Another important characteristic of the AD and unprocessed powder compacts is the formation of closed pores. The cause for the closed porosity is introduced during green fabrication itself; for example, a non-uniform powder compaction during shape forming due to irregular powder morphology of powders with wide particle size distribution. The agglomeration of AD also often results in non-uniform packing and shrinkage during firing. The non-uniform sintering and shrinkage results in the formation of stable pores at grain boundaries. As discussed earlier, during the sintering at higher temperatures, the pores cannot remain along the boundaries until they are eliminated. This pore-boundary separation forms closed pores [17]. In the processed powder compacts, better powder packing ensures a uniform sintering and results in homogeneous grain structure. The green processing is important to avert the formation of large stable pores and to increase the densification rate/coarsening rate ratio in order to readily remove finer scale porosity and prevent pore-grain boundary separation.

The SEM micrographs of the 800P sintered at 1100 °C and fracture surfaces of 800P and 1000P are shown in Fig. 4(a–d). The SEM micrograph of 800P shows a uniform equiaxial grain structure. The grain pull out observed from the fracture surface of 800P [Fig. 4(b)] clearly shows the close packing of equiaxial grains due to better green powder packing. The fracture surface of 800P and 1000P

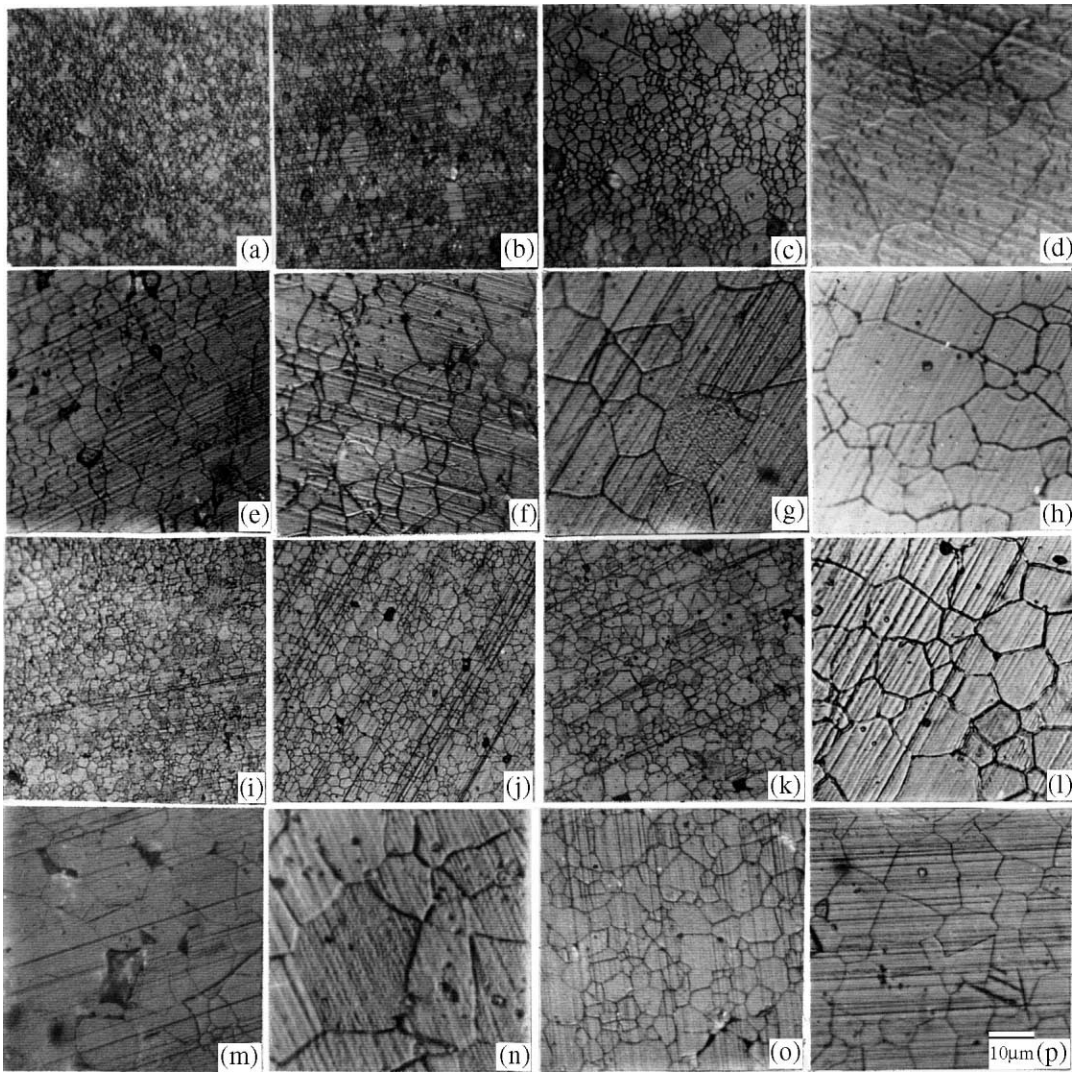

Fig. 3. Optical micrographs of HAp ceramics; AD sintered at (a) 1100, (b) 1200, (c) 1300 and (d) 1400 °C, 800C sintered at (e) 1100, (1) 1200, (g) 1300 and (h) 1400 °C, 800P sintered at (i) 1100, (j) 1200, (k) 1300 and (1) 1400 °C, 1000C sintered at (m) 1300 and (1) 1400 °C, 1000P sintered at (o) 1300 and (p) 1400 °C.

shows that the fracture mode is mainly transgranular. The fracture surface of 1000P sintered at 1300 °C shows some spherical pores along the grain boundaries.

3.4. Hardness

Fig. 5(a) shows the dependence of hardness on sintering temperature. The 800P exhibits a maximum hardness of 6.3 GPa at 1300 °C and follows a decrement at 1400 °C. The observed maximum hardness of 6.3 GPa for 800P at 1300 °C lies within the range of 5.17–6.63 GPa reported for different HAp samples sintered at temperatures ranging from 1250 to 1400 °C [18,19]. The decrease in the hardness at 1400 °C for HAp may be due to the existence of closed porosity and/or the increased grain size [20–22]. The hardness of the 1000C and 1000P are inferior to that of 800C and 800P. The lower hardness of the 1000C and 1000P samples sintered at 1200 °C is caused by the retarded densification. Fig. 5(b) shows the dependence of hardness on indentation load. Close examination of load–Vickers' hardness curves suggest a discrete transition point, where hardness changes from being load dependent to load independent. At low applied load, the indentation work is absorbed by volume deformation processes and by fracture surface formation processes. As the load is increased, the indentation becomes larger and more energy is consumed in both volume deformation and fracture surface generation processes. A number of crack types like radial, median and lateral cracks are formed during the indentation process depending upon the indenter geometry, load, elasticity and fracture toughness of the sample. In a brittle material like HAp, the fracture toughness is very low, so after the critical load (LC_1 and LC_2) the fracture surface generation processes consumes more energy and the volume deformation process is left unchanged. The

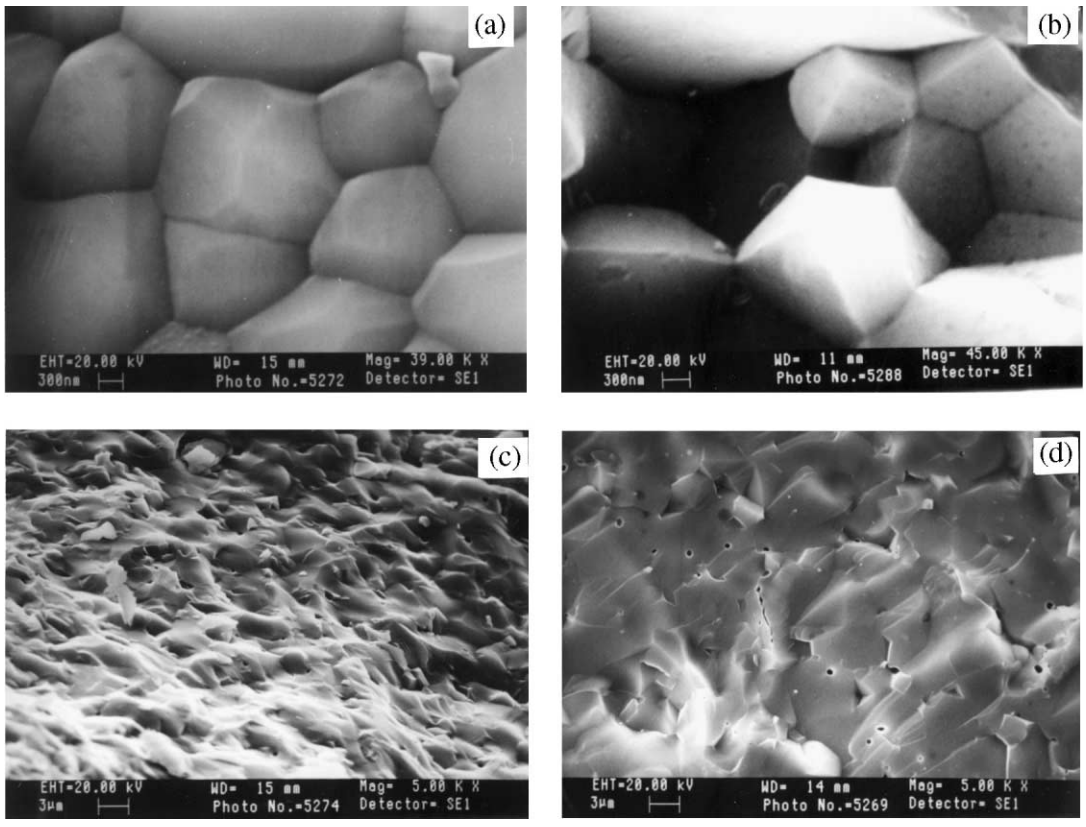

Fig. 4. SEM micrographs of (a) 800P sintered at 1100 °C, (b) grain pull out of 800P sintered at 1100 °C, (c) fracture surface of (a) and (d) fracture surface of 1000P sintered at 1300 °C.

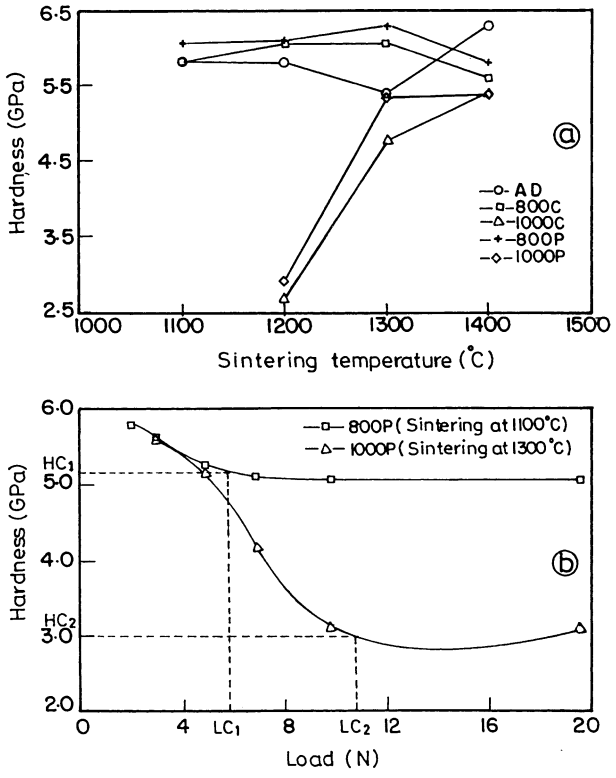

Fig. 5. Dependence of hardness of HAp on (a) sintering temperature (b) indentation load.

lower HC_2 and higher LC_2 from the curve of 1000P shows that the sample 1000P has undergone more volume deformation or plastic deformation process due to the inherent flaws, defects and pores in the material. It has been reported that the indentation size effect (ISE) changes from deformation dominated behaviour to fracture dominated behaviour above critical load levels [23–25].

3.5. Fracture toughness

Fig. 6 shows the variation of fracture toughness of the HAp samples with sintering temperature. The sample

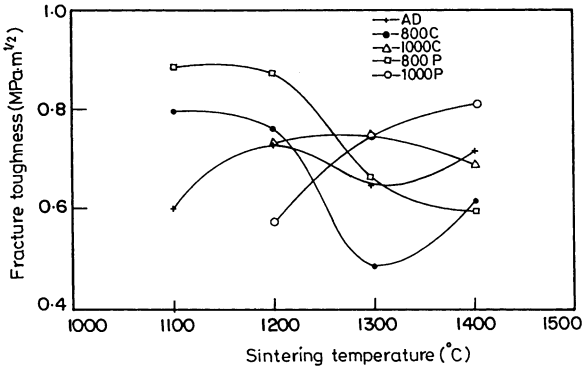

Fig. 6. Variation of fracture toughness of HAp with sintering temperature.

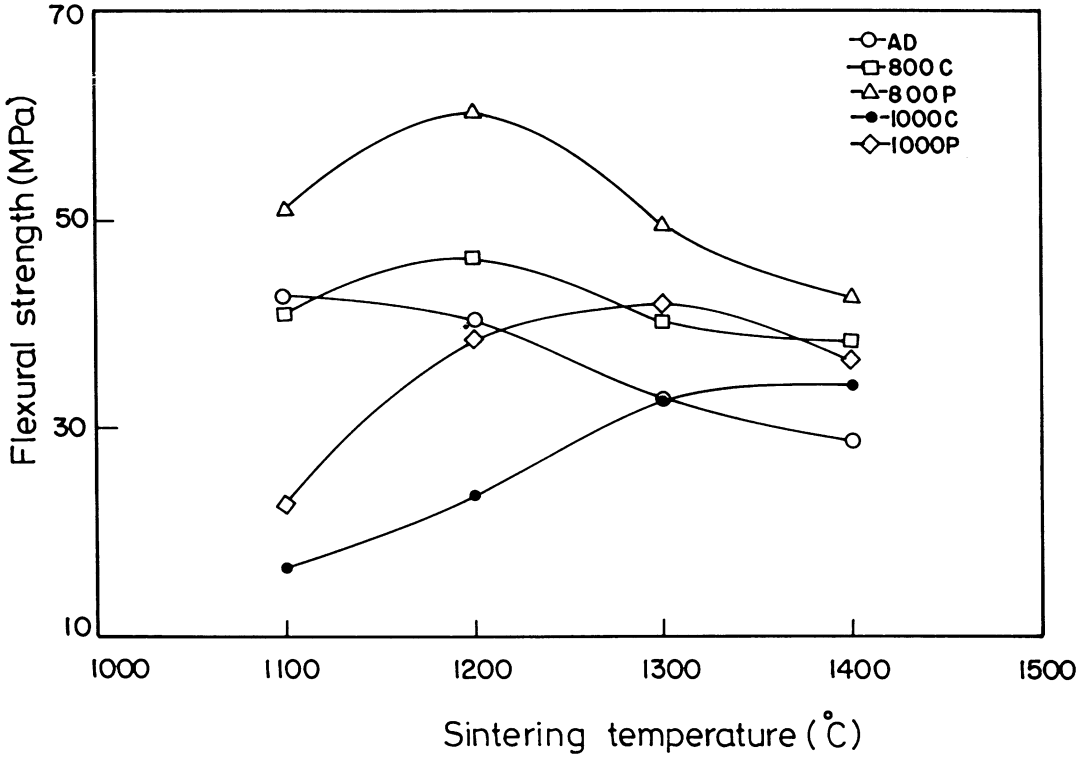

Fig. 7. Variation of flexural strength of HAp with sintering temperature.

800P shows a maximum fracture toughness of 0.88 MPa.m$^{1/2}$ at the sintering temperatures of 1100 and 1200 °C and then decreases to 0.60 MPa m$^{1/2}$ at 1400 °C. This maximum value is slightly lower than the reported K_{IC} value of 1.0 MPa.m$^{1/2}$ for HAp by Suchanek et al. [26]. The AD shows a maximum fracture toughness of 0.73 MPa m$^{1/2}$ at 1200 °C, whereas, the 800C shows an initial decrement in K_{IC} value from 0.8 to 0.49 MPa m$^{1/2}$ with increasing sintering temperatures and then increases to 0.61 MPa m$^{1/2}$. The fracture toughness of 1000P increases with increasing sintering temperature and reaches 0.8 MPa.m$^{1/2}$ at 1400 °C. The change in the fracture toughness with the sintering temperature is due to the combined influence of density and grain size. The decrement in the fracture toughness of 800P may be due to the enlarged grain size at 1300 °C. A decrease of K_{IC} with increasing grain size is usually observed in ceramics where fracture mechanism is transgranular because the major contribution to crack resistance is related to the crossing of the grain boundaries [19]. The fracture toughness of 1 000P sample has increased at 1400 °C due to the increased densification.

3.6. Flexural strength

Fig. 7 shows the variation of the flexural strength of HAp with sintering temperature. The AD sintered at 1100 °C shows a maximum flexural strength value of 42.6±6 MPa and at higher sintering temperatures the value decreases. The microstructures of the AD compact sintered at higher temperatures (>1100 °C) show abnormal and inhomogeneous grain growth which may be the reason for the strength decrement. For 800C and 800P, a maximum flexural strength of 46.2±6 and 60.3±4 MPa, respectively is observed for the samples sintered at 1200 °C. The processing of HAp has improved the packing density and sinterability of the compacts and this has resulted in a higher flexural strength for 800P; at 1300 and 1400 °C, 800P shows a decrement in the flexural strength which may be due to the grain growth. The 1000C powder compact sintered at 1400 °C shows a maximum strength of 33.9 MPa whereas, the 1000P gives a higher strength value of 41.7±5 MPa at 1300 °C itself. Even-though the processing of 1000P has improved its strength compared to 1000C, the 800P shows a better strength due to its fine grain structure. The flexural strength of HAp observed in this study is inferior to the value reported by Jarcho et al. [1] and this may be mainly due to the surface defects observed in the unpolished specimens.

4. Conclusions

The effect of powder processing on densification, microstructural development and mechanical properties of HAp compacts were studied. The 800P and 1000P compacts attained a maximum density of 97 and 97.4% of TD at the sintering temperatures of 1100 and 1300 °C, respectively. The as-dried and unprocessed powder compacts revealed a non-uniform microstructure with

abnormal grain growth and closed pores with increasing sintering temperatures. Uniform and consistent microstructures were observed for the processed powder compacts. The pore-boundary separation induced closed pores in the unprocessed compacts sintered at higher temperatures and reduced the density. The fracture mode was found to be transgranular in all the HAp ceramics.

A maximum hardness of 6.3 GPa was observed for the 800P samples sintered at 1300 °C. The load-hardness curves showed a transition point, from where the hardness becomes load dependent to load independent. The fracture toughness was calculated from the indentation crack length and a maximum toughness of 0.88 MPa $m^{1/2}$ was observed for the sample 800P sintered at 1100 °C. The 1000P showed an increasing fracture toughness value with increasing sintering temperature and at 1400 °C the value reached 0.8 MPa $m^{1/2}$. The flexural strength of HAp ceramics sintered at temperatures from 1100 to 1400 °C exhibited a maximum of 60.3 ± 4 MPa for the 800P sample sintered at 1200 °C. In general, the calcination of HAp was found to reduce the particle size, narrow its distribution and improve the microstructure and mechanical properties. Further, rehydration and milling of calcined HAp powders enhanced the microstructural homogeneity and mechanical behaviour of the sintered compact. In conclusion, HAp ceramics prepared from the processed powders (especially 800P) were found to exhibit better densification, uniform microstructure and improved mechanical properties.

Acknowledgements

One of the authors (N.T.) thanks the Council of Scientific and Industrial Research (CSIR), India for the award of a Senior Research Fellowship.

References

[1] M. Jarcho, C.H. Bolen, M.B. Thomas, J. Bobick, J.F. Kay, R.H. Doremus, Hydroxyapatite synthesis and characterization in dense polycrystalline form, J. Mater. Sci. 11 (1976) 2027–2035.
[2] I.H. Arita, D.S. Wilkinson, M.A. Mondragon, V.M. Castano, Chemistry and sintering behaviour of thin hydroxyapatite ceramics with controlled porosity, Biomaterials 16 (1995) 403–408.
[3] A.C. Tas, F. Korkusuz, M. Timuin, N. Akkal, An investigation of chemical synthesis and high temperature sintering behaviour of calcium hydroxyapatite (HA) and tricalcium phosphate (TCP) bioceramics, J. Mater. Sci.: Mater. Med. 8 (1997) 91–96.
[4] A. Royer, J.C. Viguie, M. Heughebaerl, J.C. Heughebaerk, Stoichiometry of hydroxyapatite: influence in the flexural strength, J. Mater. Sci.: Mater. Med. 4 (1993) 76–82.
[5] S. Best, W. Bonfield, Processing behaviour of hydroxyapatite powders with contrasting morphology, J. Mater. Sci.: Mater. Med. 5 (1994) 16–522.
[6] M.G.S. Murray, J. Wang, C.B. Ponton, P.M. Marquis, An improvement in processing of hydroxyapatite ceramics, J. Mater. Sci. 30 (1995) 3061–3074.
[7] A. Deptula, W. Land, T. Olezak, A. Borello, C. Alvani, A. di Bartolomea, Preparation of spherical powders of hydroxyapatite by sol–gel process, J. Non-Cryst. Solids 147 and 148 (1992) 537–541.
[8] P. Luo, T.G. Neigh, Preparing hydroxyapatite powders with controlled morphology, Biomaterials 17 (1996) 1959–1964.
[9] A.J. Ruys, M. Wei, C.C. Sorrell, M.R. Dickson, A. Brandwood, B.K. Milthrope, Sintering effects on the strength of hydroxyapatite, Biomaterials 16 (1995) 409–415.
[10] M. Aizawa, T. Hanazawa, K. Itatani, F.S. Howell, A. Kishioka, Characterization of hydroxyapatite powders prepared by ultrasonic spray-pyrolysis technique, J. Mater. Sci. 34 (1999) 2865–2873.
[11] A. Osaka, Y. Miura, K. Takeuchi, M. Asada, K. Takahashi, Calcium apatite prepared from calcium hydroxide and orthophosphoric acid, J. Mater. Sci.: Mater. Med. 2 (1991) 51–55.
[12] K. Niihara, R. Morena, D.P.H. Hasselman, Evaluation of K_1c of brittle solids by the indentations method with low crack-to-indent ratios, J. Mater. Sci. Lett. 1 (1982) 13–16.
[13] N. Thangamani, K. Chinnakali, F.D. Gnanam, The effect of calcination, rehydration and milling on the properties of hydroxyapatite powders, Biomaterials (in press).
[14] R.J. Brook, Pore–grain boundary interactions and grain growth, J. Am. Ceram. Soc. 52 (1969) 339–340.
[15] D.W. Richerson (ed.), Modern Ceramic Engineering: Properties, Processing and Use in Design, Marcel Dekker, New York, 1922.
[16] M. Hillert, Theory of normal and abnormal grain growth, Acta. Metall. 13 (1965) 227–238.
[17] R.L. Coble, J.E. Burke, Sintering in ceramics, Prog. Ceram. Sci. 3 (1963) 197–251.
[18] S. Puajindanetr, S.M. Best, W. Bonfield, Characterisation and sintering of precipitated hydroxyapatite, Brit. Ceram. Trans. 93 (1994) 96–99.
[19] P. van Landuyt, F. Li, J.P. Keustermans, J.M. Streydio, F. Delannay, E. Muting, The influence of high sintering temperatures on the mechanical properties of hydroxyapatite, J. Mater. Sci.: Mater. Med. 6 (1995) 8–13.
[20] R.W. Rice, C.C. Wu, F. Borchelt, Hardness–grain-size relations in ceramics, J. Am. Ceram. Soc. 77 (1994) 2539–2553.
[21] A. Krell, Load dependance of hardness in sintered submicrometer Al_2O_3 and ZrO_2, J. Am. Ceram. Soc. 78 (1995) 1417–1419.
[22] A. Krell, A new look at grain size and load effects in the hardness of ceramics, Mater. Sci. Eng. A245 (1998) 277–284.
[23] B.R. Lawn, T. Jensen, A. Arora, Brittleness as an indentation size effect, J. Mater. Sci. Lett. 11 (1976) 573–575.
[24] B.R. Lawn, D.B. Marshall, Hardness, toughness and brittleness: an indentation analysis, J. Am. Ceram. Soc. 62 (1979) 347–350.
[25] B.R. Lawn, A.G. Evans, D.B. Marshall, Elastic/plastic indentation damage in ceramics: the median/radial crack system, J. Am. Ceram. Soc. 63 (1980) 574–581.
[26] W. Suchanek, M. Yashima, M. Kakihana, M. Yoshimura, Hydroxyapatite/hydroxyapatite-whisker composites without sintering additives: mechanical properties and microstructural evolution, J. Am. Ceram. Soc. 80 (1997) 2805–2813.